

1 Black-box model for solar storage tanks based on multiple linear regression

2
3 Richárd Kicsiny

4
5 Department of Mathematics, Institute of Environmental Systems, Faculty of Mechanical Engineering,
6 Szent István University, Páter K. u. 1., 2100 Gödöllő, Hungary

7 E-mail address: Kicsiny.Richard@gek.szie.hu

8 Tel.: +36 28522000/1413, fax: +3628410804

10 Abstract

11 Developing easy-to-use mathematical models for describing temperatures of solar storage
12 tanks is important for the practice, since solar storages are unavoidable elements in solar
13 heating systems, where some heat should be stored in the form of hot fluid. In this paper, a
14 new, general and easy-to-apply black-box model, called LR model (where LR is the
15 abbreviation of linear regression), is proposed for solar storages on the basis of multiple
16 linear regression. This linear model may be the simplest black-box type model, which can
17 follow the transient processes of solar storages precisely. Accordingly, the LR model proves
18 to be more precise than a slightly modified version of a physically-based storage model used
19 successfully for different applications in the literature. The modified physically-based model
20 accounts for the short circuit effect occurring in storages. Comparing measured and simulated
21 data on a real solar storage, both models are validated and their efficiency is discussed in
22 details. The general and simple usability of the LR model is mentioned and future research
23 proposals are given.

24 Keywords:

25 Solar storage tanks; Modelling; Black-box; Linear regression; On/off operation

26 Nomenclature

27 t : time, s;

28 Time-dependent variables

29 T_{cold} : inlet temperature of the cold fluid to be heated in the storage, °C;

30 T_e : temperature of the environment of the storage, °C;

31 T_{in} : inlet temperature to the storage from the heating loop, °C;

32 T_{load} : temperature of the outlet fluid discharged from the storage by the consumer, °C;

33 T_s : geometrical average temperature inside the storage, °C;

34 $T_{s,meas}$: measured geometrical average temperature inside the storage, °C;

35 $T_{s,mod}$: modelled geometrical average temperature inside the storage, °C;

36 T_{out} : outlet temperature from the storage to the heating loop, °C;

37 v : pump flow rate in the heating loop (according to on/off operation), m^3s^{-1} ;

38 v_{load} : flow rate of the consumption load, m^3s^{-1}

39 Constant parameters

40 A : outside area of the storage, m^2 ;

41 c : specific heat capacity of the fluid in the storage, $\text{Jkg}^{-1}\text{K}^{-1}$;

42 c_v : modifying coefficient related to the short circuit of the heating loop inside the storage, -;
43 k : heat loss coefficient of the storage to the environment, $\text{Wm}^{-2}\text{K}^{-1}$;
44 V : volume of the storage, m^3 ;
45 ρ : mass density of the fluid in the storage, kgm^{-3} ;
46 Δt : time period between successive measurements, s;
47 τ : time delay with respect to the effects of the inlets to (the interior of) the storage, s;
48 τ_A : time lag before *Case A* in the LR model, s;
49 τ_B : time lag before *Case B* in the LR model, s

50 *Abbreviations*

51 ANN: artificial neural network;
52 CFD: computational fluid dynamics;
53 LR: linear regression;
54 MLR: multiple linear regression;
55 ODE: ordinary differential equation;
56 PDE: partial differential equation

57 **1. Introduction**

58 Developing mathematical models for describing temperatures of solar storage tanks is of
59 great importance for the practice, since these elements are unavoidable in any solar heating
60 systems, where some heat should be stored in the form of hot fluid. There are two chief kinds
61 of mathematical models of hydraulic storages: physically-based models (or white-box
62 models), describing exact physical relations (on the basis of theory) and black-box type
63 models, standing for empirical correlations based on (measured) experiences. Grey-box type
64 models are mixed versions of physically-based and black-box ones.

65 The literature contains many physically-based models. In [1], both a mixed storage model of
66 one dimension (assuming homogeneous temperature) and a multidimensional model of
67 several nodes for stratified storages are presented. In the first one-node model, an ordinary
68 differential equation (ODE), while in the latter one, a system of ODEs represent the
69 corresponding mathematical description. Zeghib and Chaker [2] propose a similar model,
70 where the storage is divided into several layers (nodes) of homogeneous temperatures, each
71 of which is represented with a single ODE.

72 If only one node is applied, we recall in essence the linear ODE model from Buzás and
73 Farkas [3]. This is one of the simplest physically-based ODE models, which can follow the
74 transient processes of solar storages with proper accuracy. This is confirmed by many works
75 showing also the successful and simple usability of the model (see e.g. [4]). Simple usability
76 is an important advantage featuring linear models. In this paper, the slightly modified version
77 of this ODE is used, which is completed with a modifying coefficient c_v responsible for the
78 so-called short circuit effect. The short circuit effect is the following: although the inlet
79 heating flow rate v can be measured, its effective value may be lower because of that a part
80 of the corresponding fluid stream flowing into the storage (from the heating loop) may
81 directly turn back and leave the storage (to the same heating loop) through the outlet pipe
82 without any heating of the bulk of the storage fluid. Based on experiences, this effect can be
83 significant and should be considered for better modelling precision. In particular, the short
84 circuit effect influences the thermal efficiency of storages [5] and, naturally, extends the
85 stagnation time of the fluid [6], which may be unhealthy in drinking water applications.

86 Temperature stratified type, heat balance, turbulent mixing and displacing mixing storage
87 models on different physical phenomena and mathematical relations with both time and space
88 dependence are summarized in [7]. The first two models are distributed ones described by

89 partial differential equations (PDEs) while the latter two ones are discretized models. A more
90 recent, dimensionless PDE model for storages of solar power plants can be found in [8].
91 CFD (computational fluid dynamics) codes for computers are important tools of realistic
92 modelling of storages [9, 10, 11, 12] using many physical equations, solving them with
93 numerical methods, but, the multistep application process of them requires expert users,
94 furthermore, their computational demand are high. In [13], the measured data and the results
95 simulated with a CFD software are compared (see Fig. 6 in [13]), based on which the
96 modelling error (the average absolute difference of the measured and simulated temperatures
97 divided by the (positive) difference between the maximal and minimal measured values) is
98 about 30% at the top of the storage and 10% in the middle. Another frequent modelling code
99 is TRNSYS, working also with numerical solution methods, which can deal with
100 stratification, internal auxiliary heating, inner heat conduction and mixing with respect to
101 storages [14].

102 The difficulties of the exact physically-based modelling caused by the complex/complicated
103 physical phenomena, like the effect of the inlet fluid flow on the thermal stratification [12,
104 15], can be often overcome by means of empirical black-box type models. The most frequent
105 black-box model version may be the artificial neural network (ANN) for thermal engineering
106 applications. Kalogirou et al. [16] model the temperature change in a solar storage with an
107 ANN with a modelling error of 7-10%. This can be called proper precision for similar
108 systems [17]. An ANN is established in [18] to predict the temperatures of the layers in a
109 storage tank for domestic water. In general, ANNs are precise tools for modelling but quite
110 arduous to use because of the so-called, quite complex and time consuming, training/learning
111 process. The uncertainty problem that there are no general and detailed algorithms for
112 designing successful ANNs, is also significant. Similar modelling tools, for example genetic
113 algorithms, can be found as well [19]. Another black-box method is given in [20], where a
114 general linear storage model is used describing the simple sum of the unperturbed process
115 and a perturbation. The coefficients in the mathematical relation are not constant but depend
116 on the so-called time shift operator.

117 Grey-box storage models are given in [21] and [22]. In the first reference, the parameter
118 values of a serial grey-box model structure are adjusted with a stochastic approximation
119 technique to simulate the oil temperature in the storage of a solar power plant. In the latter
120 work, a grey-box model and its identification procedure is presented for describing the
121 temperature of hot water tanks. The identification procedure is aimed at being a suitable tool
122 for model-based controllers.

123 Because of the above problems on arduousness and time consumption, this paper intends to
124 establish a simple, general and still precise black-box model, which can be used fast and
125 easily for a wide range of storages. This model is built on a known method of statistics,
126 namely, the multiple linear regression (MLR). After studying the literature, it can be stated
127 that MLR is a missing black-box modelling method in case of storage tanks in spite of the
128 simple applicability. MLR-based models have been worked out in recent works for other
129 working components of hydraulic heating systems, namely, for solar collectors [23] and for
130 pipes [24]. As proposing a new MLR-based storage model, called *LR model* in short, the
131 present one can be considered as the continuation of these works, in the Conclusion of which
132 it was suggested to work out MLR-based models for further elements of heating systems. The
133 contribution of the present paper is the following in details.

134 1. The linear storage model from Buzás and Farkas [3] that has been already applied
135 successfully in many works in the literature, is slightly modified (according to the short
136 circuit effect) and validated with the measurements on a real solar storage treating it as a
137 separate working component. The gained results support the practical usability of the
138 modified model (as a simple ODE) called *physically-based model* in short below.

139 2. A general, new and easy-to-apply MLR-based black-box model with low computational
 140 demand, called LR model, is proposed for solar storages. The model stands for empirical
 141 relations directly between the input variables and the storage temperature and may be the
 142 simplest possible black-box model with a rather good precision.

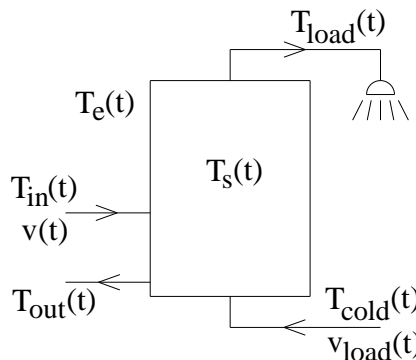
143 3. Based on measurements, the LR model is validated then compared with the physically-
 144 based model with respect to precision. The results show that the LR model is significantly
 145 more precise (with a rather low modelling error) than the physically-based model.

146 It is worth mentioning in advance that the proposed LR model is more easy-to-use and has a
 147 much lower computational demand compared to other black-box models. Furthermore, more
 148 complex models (e.g. ANNs) can have the same or even lower precision (see e.g. [17]).

149 The organization of the paper is as follows: Section 2 serves with general features on the
 150 studied solar storage type. In Section 3, the physically-based model used for comparison is
 151 introduced. The new LR model is worked out in Section 4. Based on measurements and
 152 simulated data, Section 5 details the identification and validation of the models, which are
 153 compared quantitatively in Section 6. Conclusions and future research proposals close the
 154 work in Section 7.

155 2. General features on the studied solar storages

156 Fig. 1 shows the schematic view of the studied solar storage type. The storage can be heated
 157 up through a heating loop, within which the fluid enters the storage with temperature T_{in} and
 158 leaves it with T_{out} . A pump circulates the fluid in the heating loop with 0 or a prefixed
 159 constant flow rate value v according to the on/off state of the pump. This working is in
 160 accordance with the well-known on/off control, which is likely the most widely used control
 161 method in the thermal engineering practice to date (see e.g. [25]) because of its simplicity and
 162 that this control method is the nearly optimal or even optimal one in many cases (see e.g.
 163 [26]). Sometimes a consumer discharges some fluid from the storage tank with the flow rate
 164 v_{load} . The tank, with (geometrical) average inner temperature T_s , has some heat loss to the
 165 environment through its insulation.



166
 167 Fig. 1. Schematic view of the solar storages

168 All time dependent variables T_{cold} , T_e , T_{in} , T_{load} , T_{out} , T_s , v and v_{load} are measured
 169 periodically according to a time period Δt .

170 Below, T_s denotes the geometrical average storage temperature generally, while $T_{s,mod}$ and
 171 $T_{s,meas}$ denote the modelled and measured geometrical average storage temperature,
 172 respectively.

173 3. Physically-based model

174 Eq. (1) represents the physically-based tank model used in this paper, which is the slightly
 175 modified version (completed with a modifying coefficient c_v) of the linear ODE of Buzás
 176 and Farkas [3].

$$177 \quad \frac{dT_{s,\text{mod}}(t)}{dt} = \frac{c_v v(t)}{V} (T_{in}(t) - T_{out}(t)) + \frac{v_{load}(t)}{V} (T_{cold}(t) - T_{load}(t)) + \frac{Ak}{\rho c V} (T_e(t) - T_{s,\text{mod}}(t)) \quad (1)$$

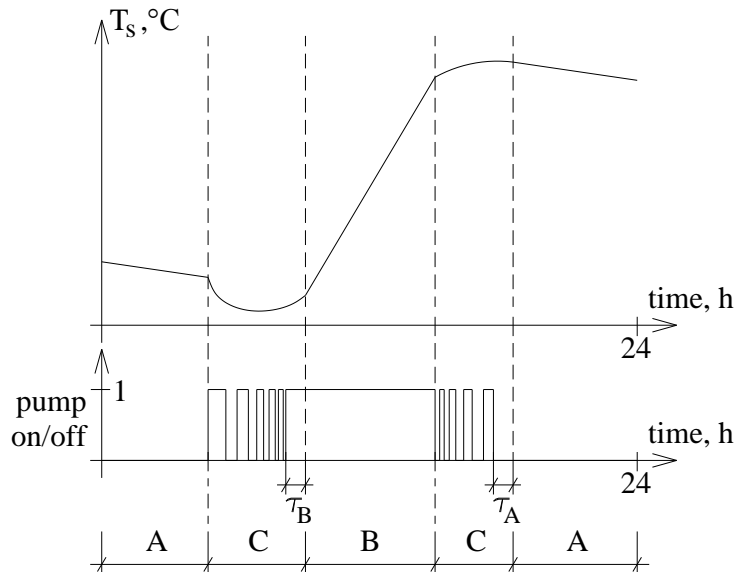
178 In Eq. (1), the short circuit effect (mentioned in the Introduction) is considered with the
 179 modifying coefficient c_v (which is between 0 and 1) for better modelling precision.

180 4. LR model

181 Because of the bounded propagation speed of physical effects and the bounded speed of
 182 measurements, the inputs of the LR model are $T_{in}(t-\tau)$, $v_{load}(t-\tau)$ and $T_s(t-\tau)$ with respect
 183 to the output (which is the modelled value of $T_s(t)$, that is, $T_{s,\text{mod}}(t)$) at the current time t .

184 Here τ is the time delay with respect to the effects of the inlets (more particularly T_{in} and
 185 v_{load}) to the interior of the storage tank. Clearly, the previously detected value of the storage
 186 temperature (as some initial value of the model) has also essential effect on its current value
 187 $T_s(t)$. For simplicity, $T_s(t-\tau)$ is taken as this previous temperature to be considered in the
 188 model.

189 Regarding the solar storage as a black-box, it can be realized that distinct sub-models should
 190 be identified as separate parts of the LR model (as a black-box model) for considerably
 191 different working conditions. More particularly, the storage tank behaves in an absolutely
 192 different way if the pump is on ($v>0$) or off ($v=0$) permanently. Namely, under the same
 193 initial tank temperature, T_s basically increases if the pump is on and decreases if the pump is
 194 off. Furthermore, the effect of T_{in} can be omitted if the pump is permanently switched off as
 195 there is no fluid flow into the tank from the heating loop then. Regarding a typical day, when
 196 the temperature increase of T_s is high enough (and the consumption load is not extremely
 197 high), three different working cases are worth distinguishing in accordance with Fig. 2.



198
 199

Fig. 2. Solar storage temperature and state of the pump on an average day

200 *Cases A and B* relate to permanently switched off and switched on pump, respectively, while
201 *Case C* relates to frequent switch-offs and -ons. The specification of all *Cases* can be found
202 below in details (see also Fig. 2).

203 *Case A*: Time of permanently switched off pump. More precisely, this *Case* contains the time
204 period, which starts at the beginning of the day and finishes at the first pump switch-on, and
205 each such time period, which starts at a time point when the pump has been continuously
206 switched off for exactly τ_A time and finishes at either the time of the next switch-on or at the
207 end of the day.

208 *Case B*: Time of permanently switched on pump. More precisely, this *Case* contains each
209 time period, which starts at a time point when the pump has been continuously switched on
210 for exactly τ_B time and finishes at the next switch-off.

211 *Case C*: This *Case* contains all time periods beyond *Cases A* and *B*. (That is, if the current
212 time point does not fit into the above conditions of *Cases A* and *B*, then it belongs to *Case C*.)

213 *Remark*

214 1. Since the fluid in the pipes of the heating loop may be colder than the storage tank at the
215 first switched on working terms of the pump, the heating loop may cool down the tank in the
216 corresponding time period (see the graph of T_s in Fig. 2 just before *Case B*).

217 2. τ_A is the time which is to be passed after a switch-off to proceed with *Case A*. More
218 particularly, τ_A is the time which is usually enough for T_s to become permanently decreasing
219 (see also Fig. 2), and, this behaviour is attributed to *Case A* as its characteristic feature.
220 Similarly, τ_B is the time which is to be passed after a switch-on to proceed with *Case B*.
221 More particularly, τ_B is the time which is usually enough for T_s to become permanently
222 increasing (see also Fig. 2), and, this behaviour is attributed to *Case B* as its characteristic
223 feature. In fact, it is subjective to some extent to determine the time point when the storage
224 temperature just begins its permanently increasing section (the end of the first section *C* in
225 Fig. 2) and the time point when the temperature just begins its permanently decreasing
226 section (the end of the second section *C* in Fig. 2), that is, to determine the value of τ_A and
227 τ_B . Nevertheless, we can estimate these values based on the (already given) measured
228 temperature graph of more days in the identification (in Section 5.1.2) then the estimated
229 daily values can be averaged, which improves the precision or, alternatively, reduces the
230 roughness of the estimate. Furthermore, rather different estimated values can serve with
231 similarly good results, because of, for example, the following effect. If τ_B is overestimated,
232 the length and significance of *Case C* clearly increases, nevertheless, the number of the time
233 points within *Case C* also increases, which will allow us in the identification process to
234 identify the model parameters with respect to *Case C* more precisely. (Similar considerations
235 hold for τ_A .)

236
237 For better modelling precision, separate sub-models are established for each working case
238 based on MLR. In the sub-models for *Cases B* and *C*, T_{in} is considered an input, since some
239 fluid flows into the storage from the heating loop according to the permanent or intermittent
240 pump working. Regarding the sub-model of *Case A*, T_{in} is omitted according to the
241 permanently switched off pump. The schemes of the MLR-based sub-models of each *Case*
242 are presented in Figs. 3 and 4.

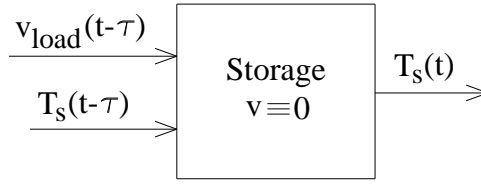


Fig. 3. Scheme of the MLR-based sub-model for *Case A*

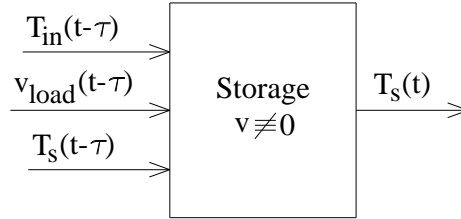


Fig. 4. Scheme of the MLR-based sub-models for *Cases B* and *C*

The LR model is formed with Eqs. (2A), (2B) and (2C), which are simple linear algebraic relations representing the corresponding sub-models of the separate working cases.

$$\text{Case A:} \quad T_{s,\text{mod}}(t) = c_{\text{load},A} v_{\text{load}}(t-\tau) + c_{s,A} T_s(t-\tau) \quad (2A)$$

$$\text{Case B:} \quad T_{s,\text{mod}}(t) = c_{\text{in},B} T_{\text{in}}(t-\tau) + c_{\text{load},B} v_{\text{load}}(t-\tau) + c_{s,B} T_s(t-\tau) \quad (2B)$$

$$\text{Case C:} \quad T_{s,\text{mod}}(t) = c_{\text{in},C} T_{\text{in}}(t-\tau) + c_{\text{load},C} v_{\text{load}}(t-\tau) + c_{s,C} T_s(t-\tau) \quad (2C)$$

$c_{\text{load},A}$, $c_{s,A}$, $c_{\text{in},B}$, $c_{\text{load},B}$, $c_{s,B}$, $c_{\text{in},C}$, $c_{\text{load},C}$ and $c_{s,C}$ are constant coefficients to be identified.

5. Identification and validation

In this section, the physically-based (Eq. (1)) and the LR (Eqs. (2A), (2B) and (2C)) model are applied to a real storage tank in order to identify and validate them. Then the efficiencies of the models are compared by means of measured and modelled data. For the calculations, the Matlab software [27] has been applied.

In the physically-based model, $T_{s,\text{meas}}(0)$ is used as initial value and the measured T_{cold} , T_e , T_{in} , T_{load} , T_{out} , v and v_{load} values are also used for solving Eq. (1) numerically to gain $T_{s,\text{mod}}(t)$. In the identification of the LR model, when the measured values of T_s can be applied, $T_{s,\text{meas}}(t-\tau)$ is used as $T_s(t-\tau)$. During the validation of the already identified LR model, the previously modelled value $T_{s,\text{mod}}(t-\tau)$ is used as $T_s(t-\tau)$ when modelling $T_s(t)$. Measured $T_{\text{in}}(t-\tau)$ and $v_{\text{load}}(t-\tau)$ values are available both during the identification and the validation. According to the specification of Δt , the measurements happen at times $t = 0, \Delta t, 2\Delta t, 3\Delta t, \dots$. Practically, the modelled value of T_s (that is $T_{s,\text{mod}}$) is determined in the LR model also at times $t = 0, \Delta t, 2\Delta t, 3\Delta t, \dots$. Furthermore, for simplicity, $\tau = \Delta t$ is assumed in the LR model. *Case A* holds and $T_s(t-\tau) = T_{s,\text{meas}}(0)$ is used as measured initial condition in Eq. (2A) at $t = \tau$ (at the beginning of the day).

The modelled real storage tank is the solar storage of a measured solar heating system [28] installed at the Szent István University (SZIU) in Gödöllő, Hungary. This storage tank will be called *SZIU storage* in short. Fig. 5 shows the photo of the SZIU storage, which contains preheated domestic water for a kindergarten at the campus of the university.



Fig. 5. SZIU storage [29]

274
275

276 The heat is transferred from a solar collector field into the SZIU storage by means of a
277 heating loop equipped with a pump working in on/off working. Since the heating loop
278 contains rather long (more than 100 metres long) pipes, the cooling down effect mentioned in
279 the *Remark* may be significant. The measurements are carried out once a minute, that is, Δt
280 $=1$ min. The volume of the SZIU storage is 2 m^3 . Based on the observation of the measured
281 storage temperature of the whole four days for the identification (see Section 5.1), τ_A and τ_B
282 are estimated 10 min (see also Note 2 in the *Remark*). These and other important parameter
283 values can be found in Table 1.

284

Table 1. Parameter values of the SZIU storage and the models

| | Physically-based model | LR model |
|---|------------------------|----------|
| A, m^2 | 4 | - |
| $c, \text{Jkg}^{-1}\text{K}^{-1}$ | 4200 | - |
| $c_v, -$ (identified) | 0.60 | - |
| $k, \text{Wm}^{-2}\text{K}^{-1}$ (identified) | 2.87 | - |
| V, m^3 | 2 | - |
| $\Delta t, \text{s}$ | 60 | 60 |
| ρ, kgm^{-3} | 1000 | - |
| τ, s | - | 60 |
| τ_A, s | - | 600 |
| τ_B, s | - | 600 |
| $c_{load,A}, \text{Ksm}^{-3}$ (identified) | - | 3.6290 |
| $c_{s,A}, -$ (identified) | - | 0.9998 |
| $c_{in,B}, -$ (identified) | - | 0.0044 |
| $c_{load,B}, \text{Ksm}^{-3}$ (identified) | - | 11.2829 |
| $c_{s,B}, -$ (identified) | - | 0.9958 |
| $c_{in,C}, -$ (identified) | - | 0.0007 |

| | | |
|---|---|---------|
| $c_{load,C}$, Ksm ⁻³ (identified) | - | 24.6179 |
| $c_{s,C}$, - (identified) | - | 0.9994 |

285 There is a temperature sensor inside the upper and another one in the lower third of the
286 storage, the values of which are averaged geometrically and considered as the measured value
287 of T_s , that is, $T_{s,meas}$. The pump flow rate v is 0 or 0.55 m³/h (based on measured data).

288 The following indices (corresponding to the currently investigated day) are used in this paper
289 for the evaluation. The *average of error* is the time average of $(T_{s,mod} - T_{s,meas})$, the *average of*
290 *absolute error* is the time average of the absolute value $|T_{s,mod} - T_{s,meas}|$. The *average of*
291 *absolute error in %* is the average of absolute error divided by the (positive) difference
292 between the (daily) maximal and minimal value of $T_{s,meas}$.

293 5.1. Identification of the models

294 For the identification, the measured data of 4 days are selected in such a way that they
295 represent a wide range of possible working conditions in a selected season (in summer). Two
296 of the days (8th June, 2012; 28th June, 2012) are with relatively high consumption load (more
297 than 1000 litres) and two ones (24th June, 2012; 2nd July, 2012) are with relatively low
298 consumption load (less than 200 litres). Based on numerous computer experiments (cannot be
299 detailed here), such 4 days has proved to be satisfactory for the identified model to have a
300 rather good accuracy. Practically, the 4 days are selected from the first third of the summer.
301 In this way, the already identified model can be conveniently used in the remaining two
302 summer months. (To apply the model for a year, the identification could be carried out for all
303 seasons separately to achieve maximal yearly precision.)

304 T_{cold} , T_e , T_{in} , T_{load} , T_{out} , v and v_{load} are assumed to be piecewise constant in the physically-
305 based model in accordance with the time step of the measurements.

306 5.1.1. Identification (physically-based model)

307 The parameters k and c_v are identified in the physically-based model. First, k is identified
308 based on such a (measured) time period when both the pump flow rate and the consumption
309 load are 0. In this case, it is assumed that the heat loss to the environment is the only
310 phenomenon which is responsible for the temperature change (decrease) of the storage, so the
311 value of k can be directly set by fitting the rate of the measured temperature decrease to the
312 rate of the modelled one. This process has been carried out based on a section of the final part
313 of the day with decreasing T_s on 2nd July, 2012. More precisely, this time period is between
314 about 18 and 21 hours on the mentioned day. See the left-hand side of Fig. 7, where it can be
315 roughly seen that the measured and modelled curves of T_s are really parallel in the
316 corresponding period. Then the value of c_v is set in such a way that the mean % value of the
317 average of absolute error is minimal with respect to the 4 identified days. The such identified
318 k and c_v values can be found in Table 1.

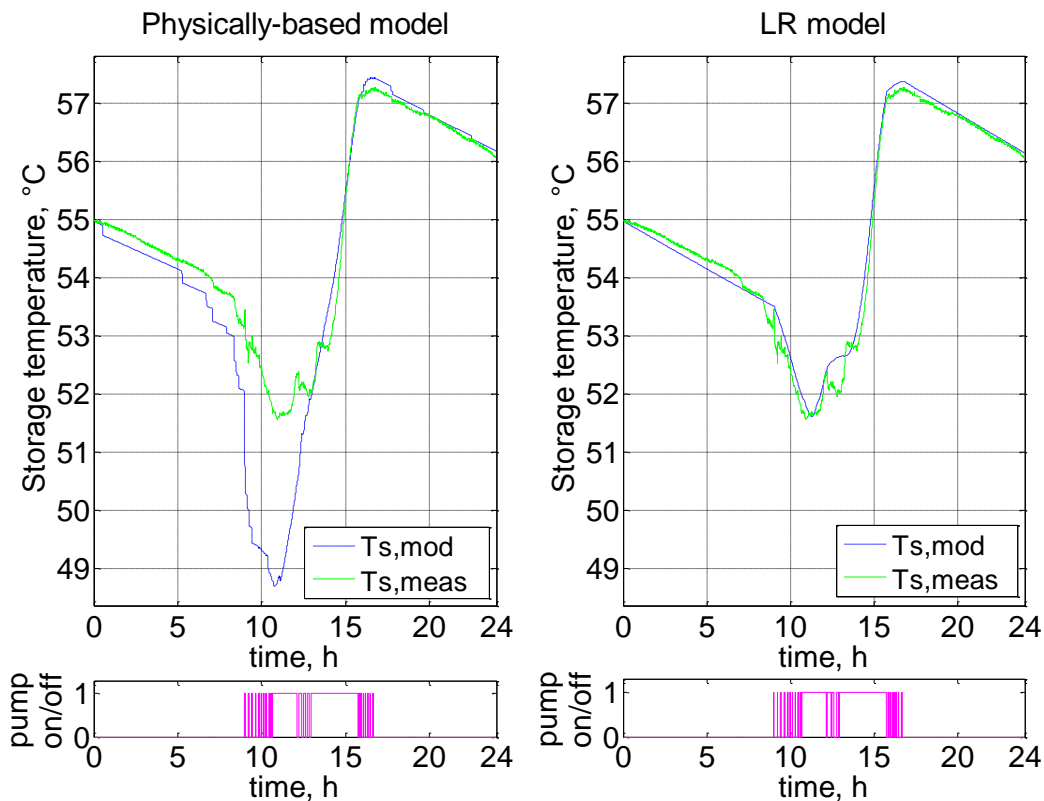
319 Table 2 presents the average of error and the average of absolute error values for two days
320 (28th June, 2012; 2nd July, 2012) of the identification (with the already identified physically-
321 based model). The average of absolute error in % is also given for both days. The mean of the
322 % values relating to all 4 days of the identification can be also seen in Table 2 (11.6 %).

323 Table 2. Average of error and average of absolute error for the models

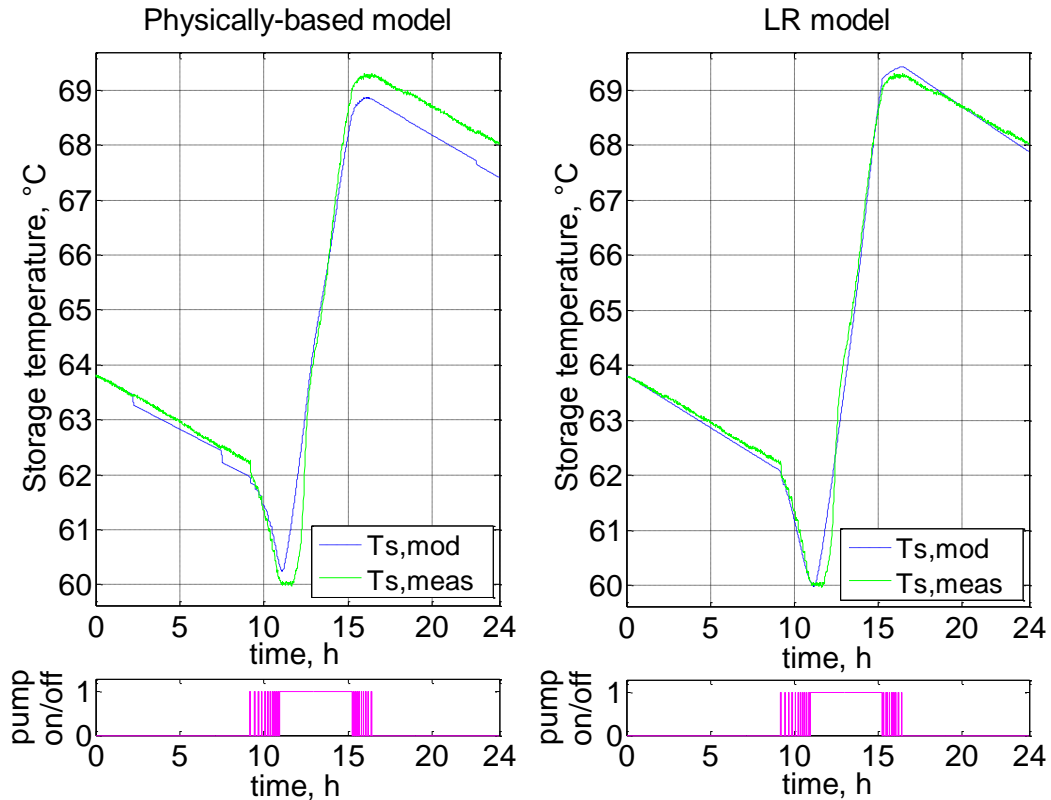
| | Physically-based model | LR model |
|--|------------------------|----------|
| | | |

| | | | | |
|--|--|---------------------------|----------------|---------------|
| Identification | 28 th June | Average of error | -0.46 °C | 0.07 °C |
| | | Average of absolute error | 0.58 °C; 10.2% | 0.15 °C; 2.7% |
| | 2 nd July | Average of error | -0.17 °C | -0.03 °C |
| | | Average of absolute error | 0.34 °C; 3.6% | 0.13 °C; 1.4% |
| Mean % value for the whole identification (4 days) | Average of absolute error | 11.6% | 2.8% | |
| Validation | 3 rd August | Average of error | 0.25 °C | -0.02 °C |
| | | Average of absolute error | 0.26 °C; 3.5% | 0.11 °C; 1.4% |
| | 5 th August | Average of error | 0.51 °C | -0.20 °C |
| | | Average of absolute error | 0.59 °C; 13.9% | 0.22 °C; 5.3% |
| | Mean % value for the whole validation (3 rd July – 31 st August) | Average of absolute error | 16.1% | 6.2% |

324 On the left-hand side of Figs. 6 and 7, the modelled and measured tank temperatures are
325 compared for two days (28th June, 2012; 2nd July, 2012) of the identification of the
326 physically-based model. The pump state (switched on or off) is also presented in both figures.



327
328 Fig. 6. Modelled $T_{s,mod}$ and measured $T_{s,meas}$ storage temperatures on 28th June, 2012 for the
329 physically-based and LR models (identification)
330



331
332 Fig. 7. Modelled $T_{s,mod}$ and measured $T_{s,meas}$ storage temperatures on 2nd July, 2012 for the
333 physically-based and LR models (identification)

334 **5.1.2. Identification (LR model)**

335 Three standard independent MLR routines are used based on the measured data of all distinct
336 working cases of the LR model (*Cases A, B, and C*) to identify parameters $c_{load,A}$, $c_{s,A}$, $c_{in,B}$,
337 $c_{load,B}$, $c_{s,B}$, $c_{in,C}$, $c_{load,C}$ and $c_{s,C}$ in Eqs. (2A), (2B) and (2C) in Section 4. For the
338 identification, the measured data of all *Cases* are selected from the same 4 identified days as
339 in case of the physically-based model in Section 5.1.1. The known standard MLR routine (on
340 the basis of least squares minimization) is built in most statistical or spreadsheet programs
341 (SPSS, Excel, etc.), so it is not needed to be detailed. The identified parameters of the LR
342 model are given in Table 1. The results of an MLR routine is generally evaluated with the
343 square of the correlation coefficient R^2 . Table 3 presents the R^2 values for all working cases
344 corresponding to the whole identification.

345 Table 3. R^2 values for the LR model

| Mode | A | B | C |
|-------|---------|---------|---------|
| R^2 | 0.99999 | 0.99998 | 0.99997 |

346 R^2 is close to 1 in all of *Cases A, B* and *C*, because of which the LR model can be considered
347 very reasonable. The indices of Table 2 are more expressive and more important, especially,
348 in the aspect of the comparison with the physically-based model applied already successfully
349 in the literature. Table 2 presents the average of error and the average of absolute error values
350 for two days (28th June, 2012; 2nd July, 2012) of the identification (with the already identified
351 LR model). The average of absolute error in % is also given for both days. The mean of the
352 % values relating to all 4 days of the identification can be also seen in Table 2 (2.8 %).

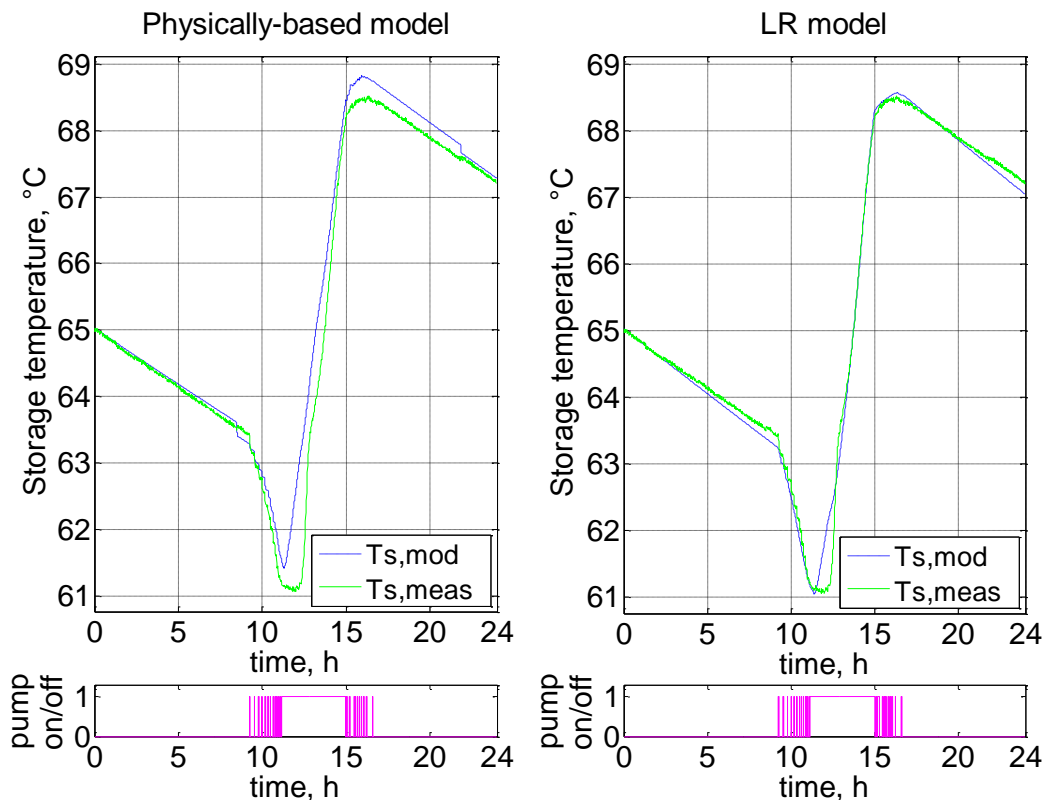
353 On the right-hand side of Figs. 6 and 7, the modelled and measured tank temperatures are
 354 compared for two days (28th June, 2012; 2nd July, 2012) of the identification of the LR model.
 355 The working state of the pump is also presented in the figures.

356 5.2. Validation of the models

357 For validation, the identified physically-based model and the identified LR model are used
 358 with the proper measured inputs from the remaining two months of the summer. More
 359 precisely, one of the inputs of the LR model is changed compared to the inputs of the
 360 identification, that is, the modelled $T_{s,mod}(t-\tau)$ is applied as $T_s(t-\tau)$ in the LR model (2A),
 361 (2B) and (2C) (not $T_{s,meas}(t-\tau)$). The modelled period for the validation, from 3rd July, 2012
 362 to 31st August, 2012, contains 56 days (according to some short technical interruptions).

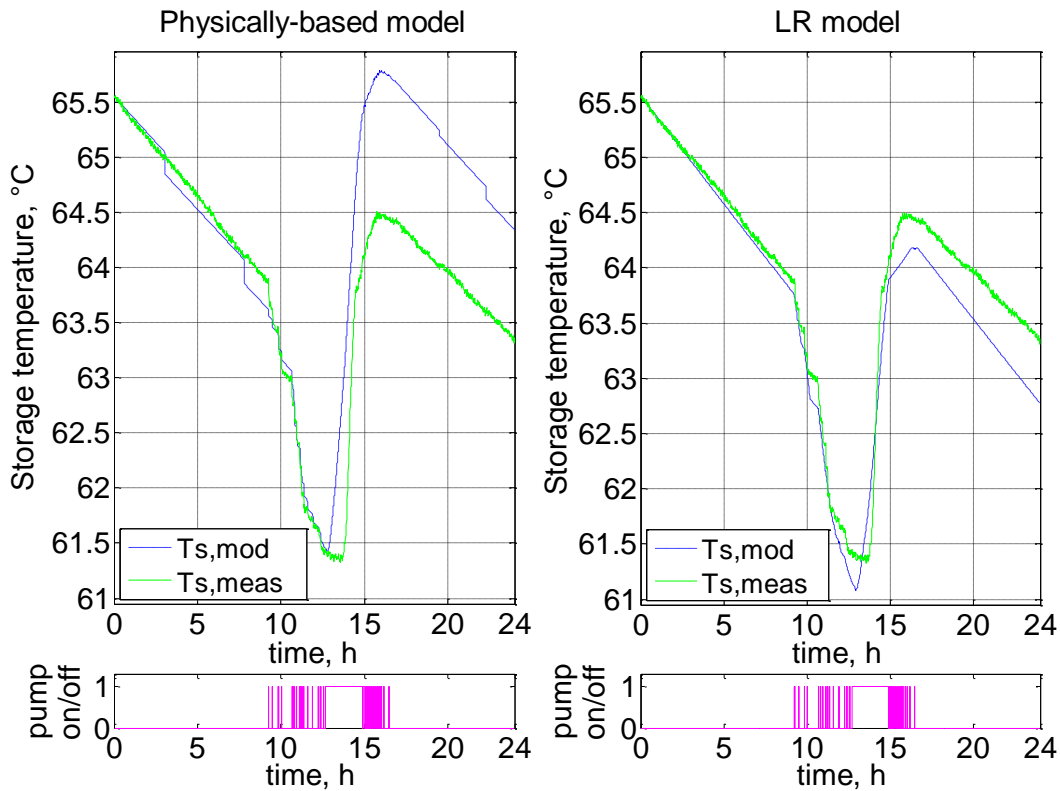
363 The modelled and the measured storage temperatures are compared and evaluated in case of
 364 the two models. Table 2 presents the average of error and the average of absolute error values
 365 for two days (3rd August, 2012; 5th August, 2012) of the validation for the models. The
 366 average of absolute error in % is also given for both days. The mean of the % values relating
 367 to the whole time period of 3rd July – 31st August can be also seen in Table 2 (16.1% and
 368 6.2% for the physically-based and LR models, respectively).

369 In Figs. 8 and 9, the modelled and measured tank temperatures are compared in case of both
 370 models for two days (3rd August, 2012; 5th August, 2012) of the validation. The pump state is
 371 also presented in both figures.



372
 373 Fig. 8. Modelled $T_{s,mod}$ and measured $T_{s,meas}$ storage temperatures on 3rd August, 2012 for the
 374 physically-based and LR models (validation)

375



376
 377 Fig. 9. Modelled $T_{s,mod}$ and measured $T_{s,meas}$ storage temperatures on 5th August, 2012 for the
 378 physically-based and LR models (validation)

379 **6. Comparison and discussion**

380 The LR model can predict the storage temperature rather precisely, particularly, more
 381 precisely than the physically-based model. According to the validation, the mean (absolute)
 382 modelling error (in %) is 6.2% with the LR model and 16.1% with the physically-based
 383 model. The latter has been already used successfully in many works in the literature. Thus the
 384 accuracy of the LR model can be stated very well regarding general solar thermal engineering
 385 purposes (studying and developing the thermal processes of solar storages).

386 In addition, the R^2 values between the modelled and measured data with respect to the above
 387 selected 4 days (2 identified and 2 validated ones) have been determined for the models. They
 388 are given in Table 4 confirming the better precision of the LR model compared to the
 389 physically-based one.

390 Table 4. R^2 values for the models for whole days

| Date | 28 th June, 2012 (identification) | 2 nd July, 2012 (identification) | 3 rd August, 2012 (validation) | 5 th August, 2012 (validation) |
|------------------------|---|--|--|--|
| Physically-based model | 0.918 | 0.990 | 0.976 | 0.713 |
| LR model | 0.988 | 0.995 | 0.994 | 0.965 |

391 It should be mentioned that the storage temperature cannot be expected to be predicted
 392 perfectly with relatively simple models, largely because of the above discussed short circuit
 393 effect. This effect must be rather complex, and thus hard to model, depending on the current
 394 flow rate values v , v_{load} and, probably, on the different temperature values of the system. In
 395 case of the SZIU storage, v is relatively high ($0.55 \text{ m}^3/\text{h}$) compared to the tank volume (2
 396 m^3), which likely makes the short circuit effect significant. It should be also mentioned that

397 neither model takes into account the thermal stratification inside the storage, which must be
398 more disadvantageous for the physically-based model than for the LR model, since the
399 strength of black-box models is just that they can often serve with rather precise empirical
400 relations without dealing with the physical backgrounds. These must be the reason for that
401 the accuracy of the physically-based model is not outstanding (the error is over 10%). On the
402 other hand, these difficulties also confirm the reasonability and robustness of the LR model
403 considering that its error is rather low (close to 5% in the validation). In sum, the accuracy of
404 the LR model can be stated very well, especially, regarding its simplicity. Furthermore, the
405 physically-based model can be stated still usable in the practice as a simple ODE model (c.f.,
406 for example, the 30% and 10% error values reported in [13] in the Introduction).
407 In fact, there are more parameters to be identified in the LR model than in the physically-
408 based model, but, on the whole (and even in the identification), it is much easier and faster to
409 apply the LR model, since it means only one explicit algebraic operation at each minute (each
410 time step) as it is a simple algebraic equation (depending on the current *Case*), while the
411 physically-based model is a differential equation, which must be discretized then solved
412 numerically. Generally, at least 100 time steps is suggested per minute for a satisfactorily
413 precise numerical calculation, which means at least 100 times more algebraic operations than
414 in case of the LR model.

415 **7. Conclusions**

416 The purpose of the present research was to work out a general, easy-to-apply but still precise
417 mathematical model for solar storages. After studying the literature, it can be stated that MLR
418 is a missing black-box modelling method in case of hydraulic storage tanks in spite of the
419 (linear algebraic) simplicity. In this paper, a new model, called LR model, has been
420 established and validated based on measured data to fulfil this research gap. The proposed LR
421 model may be the simplest possible black-box model with a rather low modelling error (close
422 to 5%, more precisely, 6.2%) and with very low computational demand.

423 The slightly modified version of the physically-based linear ODE model of Buzás and Farkas
424 [3] for solar storages has been validated as well with a modelling error of 16.1%. This model
425 accounts for the short circuit effect in storage tanks.

426 Considering the complex, and hard to predict, short circuit effect of the modelled solar
427 storage (the SZIU storage), the accuracy and the robustness of the LR model can be stated
428 very well, furthermore, the physically-based model is still usable in the practice as a simple
429 ODE model. It is not difficult to think that both models would be even more accurate in case
430 of a more regular tank (with less significant short circuit effect).

431 After assigning *Cases A, B* and *C*, it is not difficult to identify the LR model (2A), (2B) and
432 (2C) for any storage tanks according to the identification method of Section 5.1.2 (in case of
433 similar inputs and output as there), so the LR model is also general.

434 Basically, the LR model can be used for very fast but still precise storage
435 modelling/simulation, nevertheless, because of its simple linear algebraic equations, the
436 computational demand is very low, which may make it convenient for model-based control
437 schemes. The advantage of the simple usability and the low computational demand can be
438 seen especially compared to other, more complex black-box type models having essentially
439 the same or even lower precision.

440 MLR-based models have been worked out in recent works for other working components of
441 hydraulic heating systems, namely, for solar collectors [23] and for pipes [24]. The LR model
442 can be considered as the continuation of these works, in the Conclusion of which it was
443 suggested to work out MLR-based models for further elements (like storage tanks) of
444 hydraulic heating systems.

445 Future researches may deal with connecting the already worked out MLR-based models of
446 the separate working components to form an easy-to-use and precise MLR-based model for

447 complete solar heating systems. Furthermore, new model-based controls could be created on
448 the basis of the LR model.

449 **Acknowledgement**

450 The author thanks the Editor for the help in submitting the paper, the Department of Physics
451 and Process Control in the Faculty of Mechanical Engineering (SZIU) for the measured data
452 of the SZIU storage and his colleagues, especially Éva Dékány, in the Department of
453 Mathematics for the support.

454 This paper was supported by the János Bolyai Research Scholarship of the Hungarian
455 Academy of Sciences.

456 **References**

- 457 [1] Duffie JA, Beckman WA (2006) Solar engineering of thermal processes, 3rd edn. John Wiley and
458 Sons, New York
- 459 [2] Zeghib I, Chaker A (2011) Simulation of a solar domestic water heating system. *Energy Procedia*
460 6:292-301.
- 461 [3] Buzás J, Farkas I (2000) Solar domestic hot water system simulation using blockoriented software.
462 In: The 3rd ISES-Europe solar world congress (Eurosun 2000), Copenhagen, Denmark, CD-ROM
463 Proceedings, p. 9.
- 464 [4] Kumar R, Rosen MA (2010) Thermal performance of integrated collector storage solar water
465 heater with corrugated absorber surface. *Appl Therm Eng* 30:1764-1768.
- 466 [5] Jannatabadi M, Taherian H (2012) An experimental study of influence of hot water consumption
467 rate on the thermal stratification inside a horizontal mantle storage tank. *Heat Mass Transf*
468 48(7):1103-1112.
- 469 [6] Duer M (2011) Passive mixing systems improve storage tank water quality. *Opflow* 37(8):20-23.
- 470 [7] Han YM, Wang RZ, Dai YJ (2009) Thermal stratification within the water tank. *Renew*
471 *Sustainable Energy Rev* 13:1014-1026.
- 472 [8] Bayón R, Rojas E (2013) Simulation of thermocline storage for solar thermal power plants: From
473 dimensionless results to prototypes and real-size tanks. *Int J Heat Mass Transfer* 60:713-721.
- 474 [9] Altuntop N, Arslan M, Ozceyhan V, Kanoglu M (2005) Effect of obstacles on thermal
475 stratification in hot water storage tanks. *Appl Therm Eng* 25:2285-2298.
- 476 [10] Zachár A, Aszódi A (2007) Numerical analysis of flow distributors to improve temperature
477 stratification in storage tanks. *Numer Heat Tr A-Appl* 51:919-940.
- 478 [11] Zachár A (2013) Investigation of a new tube-in-tube helical flow distributor design to improve
479 temperature stratification inside hot water storage tanks operated with coiled-tube heat exchangers.
480 *Int J Heat Mass Transfer* 63:150-161.
- 481 [12] Wang Z, Zhang H, Dou B, Huang H, Wu W, Wang Z (2017) Experimental and numerical
482 research of thermal stratification with a novel inlet in a dynamic hot water storage tank. *Renew*
483 *Energy* 111:353-371.
- 484 [13] Johannes K, Fraisse G, Achard G, Rusaouën G (2005) Comparison of solar water tank storage
485 modelling solutions. *Sol Energy* 79:216-218.
- 486 [14] Klein SA et al. (2005) TRNSYS 16 – A transient system simulation program. Solar Energy
487 Laboratory, University of Wisconsin-Madison
- 488 [15] Meyer JP, Raubenheimer PJA, Kruger E (2000) The influence of return loop flow rate on
489 stratification in a vertical hot water storage tank connected to a heat pump water heater. *Heat*
490 *Transfer Eng* 21(2):67-73.
- 491 [16] Kalogirou SA, Panteliou S, Dentsoras A (1999) Modelling of solar domestic water heating
492 systems using artificial neural networks. *Sol Energy* 65(6):335-342.
- 493 [17] Kalogirou SA (2000) Applications of artificial neural-networks for energy systems. *Appl Energy*
494 67:17-35.
- 495 [18] Géczy-Víg P, Farkas I (2010) Neural network modelling of thermal stratification in a solar DHW
496 storage. *Sol Energy* 84:801-806.
- 497 [19] Cabello JM, Cejudo JM, Luque M, Ruiz F, Deb K, Tewari R (2011) Optimization of the size of a
498 solar thermal electricity plant by means of genetic algorithms. *Renew Energy* 36(11):3146-3153.

- 499 [20] Romero JA, Navarro-Esbri J, Belman-Flores JM (2011) A simplified black-box model oriented
500 to chilled water temperature control in a variable speed vapour compression system. *Appl Therm*
501 *Eng* 31:329-335.
- 502 [21] Arahall MR, Cirre CM, Berenguel M (2008) Serial grey-box model of a stratified thermal tank for
503 hierarchical control of solar plant. *Sol Energy* 82:441-451.
- 504 [22] De Ridder F, Coomans M (2014) Grey-box model and identification procedure for domestic
505 thermal storage vessels. *Appl Therm Eng* 67(1-2):147-158.
- 506 [23] Kicsiny R (2016) Improved multiple linear regression based models for solar collectors. *Renew*
507 *Energy* 91:224–232.
- 508 [24] Kicsiny R (2017) Grey-box model for pipe temperature based on linear regression. *Int J Heat*
509 *Mass Transfer* 107:13–20.
- 510 [25] Araújo A, Pereira V (2017) Solar thermal modeling for rapid estimation of auxiliary energy
511 requirements in domestic hot water production: On-off flow rate control. *Energy* 119:637-651.
- 512 [26] Winn CB, Hull DE (1979) Optimal controllers of the second kind. *Sol Energy* 23:529-534.
- 513 [27] Etter DM, Kuncicky D, Moore H (2004) *Introduction to MATLAB 7*. Springer
- 514 [28] Farkas I, Buzás J, Lágymányosi A, Kalmár I, Kaboldy E, Nagy L (2000) A combined solar hot
515 water system for the use of swimming pool and kindergarten operation. *Energy and the*
516 *environment*, Vol. I. /ed. by Frankovic B/, Croatian Solar Energy Association, Opatija, 2000., 81-
517 88.
- 518 [29] Géczyné Vig P (2007) Modelling of solar heating systems with neural network. Dissertation,
519 Szent István University, Gödöllő, p. 130. [in Hungarian]
520 https://szie.hu/file/tti/archivum/geczine_v_p_phd.pdf Accessed 10 August 2017